Polymer Crystallites with Few Tie Molecules from a Miscible Polymer Blend

Yongjin Li,* Yuko Iwakura, and Hiroshi Shimizu

Nanotechnology Research Institute, National Institute of Advanced Industrial Science and Technology (AIST), Tsukuba Central 5, 1-1-1 Higashi, Tsukuba, Ibaraki 305-8565, Japan

Received January 22, 2008
Revised Manuscript Received March 21, 2008

Introduction. It is generally accepted that the presence of molecular connections between different crystallites, namely, tie molecules, takes the key role in determining the mechanical performance of semicrystalline polymers.[1–4] If the tie molecules did not exist, the polymer crystallites would only be held together by van der Waals or hydrogen bond interactions. These physical interactions are obviously too weak to provide sufficient strength for connecting adjacent crystallites under stress, and this results in the macroscopic brittleness and low strength of the material. The formation of tie molecules has been attributed to the random coil dimension in the molten state being larger than the thickness of crystallite formed in the solidified state after crystallization.[5–7] Several crystalline lamellae can grow within the sphere of gyration of a chain as long as the molecular chain is sufficiently long. Therefore, the long chain molecule can cross the amorphous layer and provide the mechanical bridging of the adjacent crystalline lamellae. Because of the great importance of the tie molecules for the properties of semicrystalline polymers, numerous investigations have been carried out to assess the concentration of tie molecules and to evaluate the effects of the concentration on the mechanical properties of materials.[8–12] Although the concentration of tie molecules can be adjusted by changing the molecular structure and/or varying the crystallization conditions,[13–17] the polymer crystals with very few tie molecules are difficult to prepare from melt for high molecular polymers due to the molecular entanglement in the bulk state. However, it is obvious that the preparation of polymer crystals with very few (or even no) tie molecules and the investigation of the crystallization behavior of these crystals are very important from both academic and industrial points of view.

Miscible crystalline/amorphous polymer blends can form various types of crystalline morphology depending on the location of molecular chains of the amorphous component.[18–20] We consider that the interlamellar structure,[21–23] where the molecular chains of the amorphous component are inserted into the lamellar gallery of the crystalline component, provides a good platform for manipulating the tie molecule concentration. The molecular chain incorporation of the amorphous component into the interlamellar area will not only increase the distance between the adjacent lamellae but also decrease the crystalline component concentration in the amorphous region. Thus, the tie molecule concentration decreases gradually with the insertion of the amorphous component and polymer crystallites will finally be isolated by the molecular chains of the amorphous component at a critical point. However, almost all the miscible crystalline/amorphous polymer blends show melting temperature depression and crystallinity reduction with increasing the amorphous polymer content.[18–25] Therefore, the crystalline component usually becomes noncrystallizable before reaching this critical point in most cases. In this Communication, we have successfully prepared the poly(vinylidene fluoride) (PVDF) crystals with few tie molecules from its miscible blend with acrylic rubber (ACM). Neither melting temperature depression nor crystallinity reduction was observed for this miscible blend where ACM is the dominant component. ACM molecular chains are inserted into the amorphous region of PVDF lamellae, and PVDF crystallites are isolated from each other by the ACM molecules. The orientation behaviors of this type of crystals upon stretching have been compared with the crystals in neat PVDF where many tie molecules connect the neighbor crystals. To our best knowledge, this is the first report on the polymer crystallites with very few tie molecules from the melt for a high molecular weight commercial polymer.

Experimental Section. The PVDF and ACM samples used were commercially available KF850 (Kureha Chemicals, Japan) and AR32 (Nippon Zeon Co., Ltd.), respectively. The molecular weight and polydispersity of the PVDF, determined by gel permeation chromatography, are $M_w = 209\,000$ and $M_w/M_n = 2.0$, respectively. Those for the ACM are $M_w = 656\,000$ and $M_w/M_n = 11.7$. All the polymers were dried in a vacuum oven at 80 °C for at least 12 h before processing. Blends with an ACM component concentration of more than 70 wt % were prepared using a Brabender-type plastic mixer (Toyoseiki Co. KF70V) with two rotors at a rotation speed of 100 rpm at 190 °C for 10 min. After blending, all the samples were hot pressed at 200 °C for 5 min into a film with a thickness of 500 μm, followed by quenching in ice−water. The obtained films were used for further characterization.

The miscibility was characterized by dynamic mechanical analysis (DMA), which was carried out with a RHEOVIBRON DDV-25FP (Orientec Corp.) in tensile mode. The dynamic storage and loss moduli were determined at a frequency of 1 Hz and a heating rate of 3 °C/min as a function of temperature from −150 to 150 °C. Differential scanning calorimetry (DSC) was carried out under nitrogen flow at a heating or cooling rate of 10 K/min with a Perkin-Elmer DSC-7 differential scanning calorimeter calibrated using the melting temperatures of indium and zinc. The PVDF crystal in the blends was observed directly using a transmission electron microscopy (TEM) (Hitachi H7000) operating at an acceleration voltage of 75 kV. The blend samples were ultramicrotomed at −120 °C to a section with a thickness of about 70 nm. The sections were then stained with RuO_4 for 20 min. Small-angle X-ray scattering (SAXS) patterns were obtained by microfocused Cu Kα radiation (45 kV, 60 mA) generated by an X-ray diffractometer (Rigaku Ultrax 4153A 172B) and an imaging plate detector. Wide-angle X-ray diffraction (WAXD) profiles were obtained using Cu Kα radiation (40 kV, 120 mA) generated by an X-ray diffractometer (Rigaku, Ultrax 8000) with a scanning speed of 1 deg/min. WAXD patterns for the stretched samples were obtained using the same X-ray diffractometer with an imaging plate detector. Tensile test was carried out according to the ASTM D 412-80 test method using dumbbell-shaped samples to obtain stress−strain curves.

Results and Discussion. PVDF and ACM are miscible in the composition range investigated here, as confirmed by the measurements of the glass transition temperature (T_g) of blends using DMA. Only one T_g is observed for the all blends, and the measured T_g is highly consistent with the theoretical T_g calculated by the Fox equation (see Figures S1 and S2 in the Supporting Information). The miscibility is attributed to the specific interactions between CF_2 groups of PVDF and carboxyl groups of ACM, similar to that for the blend of PVDF with poly(methyl methacrylate) (PMMA).[24,26] Although all the blends

* To whom correspondence should be addressed. E-mail: yongjin-li@aist.go.jp.

10.1021/ma800148x CCC: $40.75
Published on Web 04/29/2008

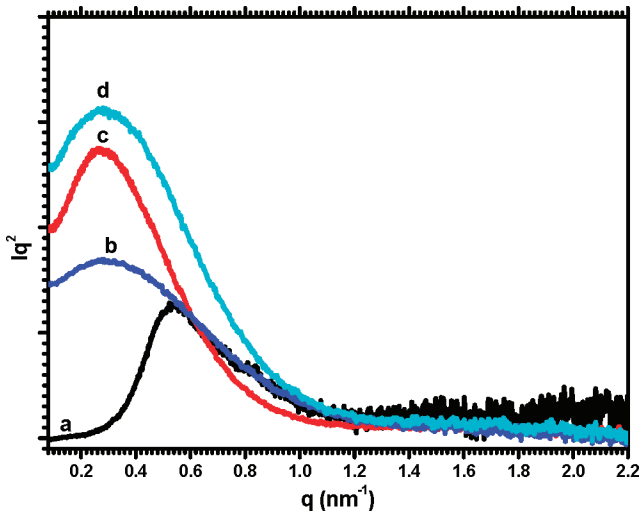

Figure 1. Lorentz-corrected SAXS profiles for (a) neat PVDF, (b) ACM/PVDF = 90/10, (c) ACM/PVDF = 80/20, and (d) ACM/PVDF = 70/30.

investigated here are ACM-rich, PVDF can still crystallize well from the miscible blends. DSC investigation indicates that neither melting temperature (T_m) depression nor crystallinity reduction occurs for this miscible crystalline/amorphous polymer blend. However, the PVDF crystallization rate is significantly reduced by the addition of high content amorphous ACM (see Figure S3 and Table S1 in the Supporting Information). Generally, miscible blends having favorable but not strong interactions display small T_m depression for the polymers having very close chemical nature,[27,28] while large T_m depression and crystallinity reduction are found for the miscible blends with strong molecular interactions.[24,29] The phenomena observed here are pretty unusual. We consider that ACM molecules act as a good macromolecular diluent for PVDF but show almost no thermodynamic influence for the crystallization of PVDF. Obviously, although the carboxyl groups in ACM molecular chain have specific interaction with CF_2 groups in PVDF, this interaction would be much weaker than that in PMMA and PVDF since ACM contains lower carboxyl groups as a copolymer. On the other hand, the decreased crystallization rate for PVDF in the blends can be attributed to the protracted transport process for the PVDF segments during crystallization because of the lowering concentration of PVDF chains in the blends.

Figure 1 displays the Lorentz-corrected SAXS profiles of neat PVDF and the PVDF/ACM blends. The SAXS intensity was normalized by thickness and exposure time after subtracting air scattering from the observed profiles. Neat PVDF exhibits a weak scattering peak at $q = 0.55$ nm^{-1}, corresponding to a crystal long period of 11.4 nm. On the other hand, the PVDF/ACM (70/30) blend shows a very strong scattering peak at $q = 0.25$ nm^{-1}, corresponding to a crystal long period of 25.1 nm. The significantly increased crystal long period indicates that a large number of ACM molecular chains were incorporated into the gallery of PVDF lamellae in the blend. This is further proved by the enhancement of scattering intensity for the blend as compared with that for neat PVDF. Since the electron density of ACM is much lower than that of the amorphous PVDF, the insertion of ACM between individual PVDF lamellae would inevitably enhance the electron density contrast between the crystalline and amorphous layers and consequently results in higher scattering intensity. The crystal long period remains almost constant with increasing ACM content in the blends

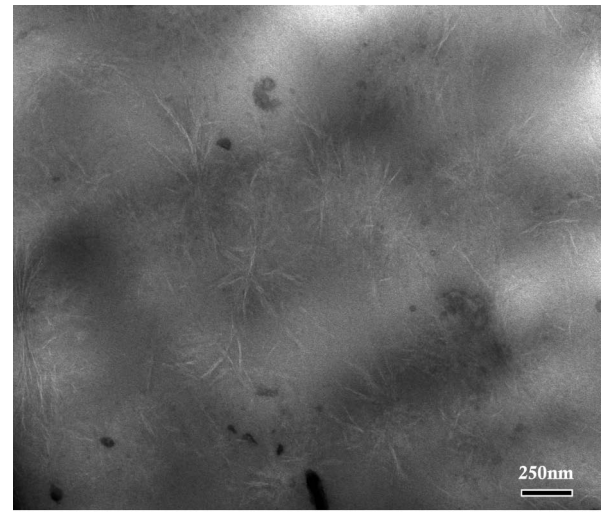

(a)

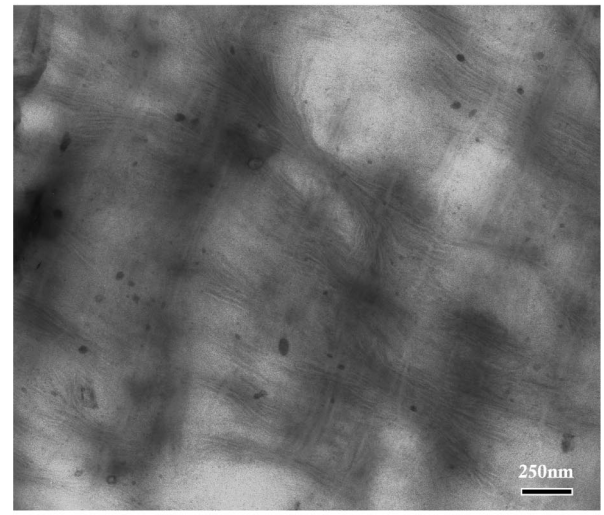

(b)

Figure 2. TEM micrographs of PVDF crystallites in (a) PVDF/ACM = 10/90 and (b) PVDF/ACM = 30/70.

investigated here, but the SAXS scattering intensity decreases continuously with increasing ACM content from 70% to 90%. This can be attributed to the decreased crystalline fraction in the blends upon increasing ACM content.

The crystallized PVDF lamellae from the miscible blends have been directly observed using TEM, as shown in Figure 2. PVDF lamellae can be very clearly observed in all blends. However, no lamellae can be observed for neat PVDF using the same staining method (TEM image for neat PVDF not shown here). This difference again suggests the incorporation of ACM molecular chain into the gallery of PVDF lamellae. Since ACM is more easily stained by RuO_4 than PVDF, the insertion of ACM chain between the PVDF lamellae can increase the contrast between the amorphous part and the crystalline region in the blends. Although PVDF content in the blend is very low, the PVDF crystals can be clearly observed. The long period of the crystal lamellae from the TEM observation is about 20−25 nm, which is consistent with the value obtained from the SAXS measurements.

The markedly increased crystal long period caused by the incorporation of amorphous ACM chains between the adjacent crystallites is thought to significantly decrease the number of PVDF tie molecules, which may greatly affect the orientation behaviors of the formed crystals. Figure 3 shows the WAXD

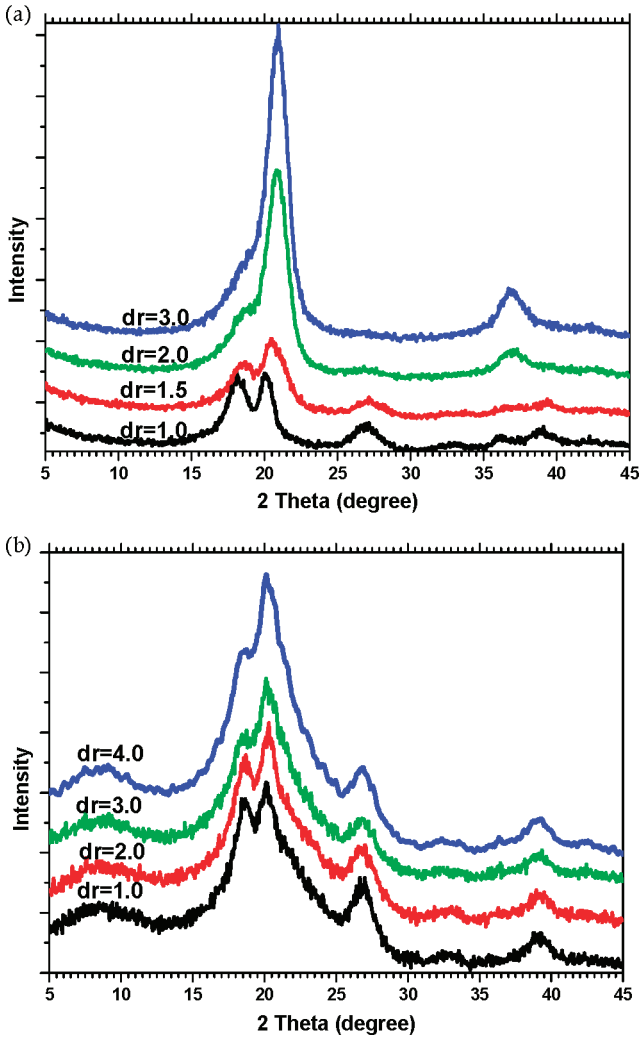

Figure 3. WAXD profiles for (a) neat PVDF and (b) PVDF/ACM = 30/70 blend with the indicated draw ratio.

profiles of neat PVDF and the PVDF/ACM = 30/70 blend after stretching with the indicated draw ratios. Note that the PVDF/ACM = 20/80 and PVDF/ACM = 10/90 blends show the same behavior as the PVDF/ACM = 30/70 sample. For neat PVDF, it is seen that the typical α-phase before stretching is transformed into the β-phase with increasing draw ratio. This is the well-known mechanical deformation induced crystal form transition behavior for PVDF.[30–33] In contrast, for the PVDF crystals in the PVDF/ACM blends investigated here, all the blends with different draw ratios show the same WAXD reflections, which are the typical PVDF α-phase reflections. In other words, different from neat PVDF, no strain-induced phase transition can be observed for the blends investigated here.

Figure 4 shows the azimuthal profile of the (110)/(020) (2θ = 20.5°) reflection in neat PVDF and that of the (020) (2θ = 18.8°) reflection in the PVDF/ACM blends with a draw ratio of 4.0 as well as the 2-dimensional WAXD patterns. For neat PVDF, the strong and sharp reflection spots corresponding to the (110)/(020) reflections of PVDF β-phase (at 2θ = 20.5°) were observed, indicating the formation of fibrillar structure by the mechanical deformation. The fact that the reflection spots are only located on the equator in the WAXD pattern and the maximum reflection intensity appears at ϕ = 90° and 270° in the azimuthal profile demonstrates that the molecular chains in the formed crystal blocks are rendered to align along the stretch direction (*c*-axis orientation). For the PVDF/ACM blend

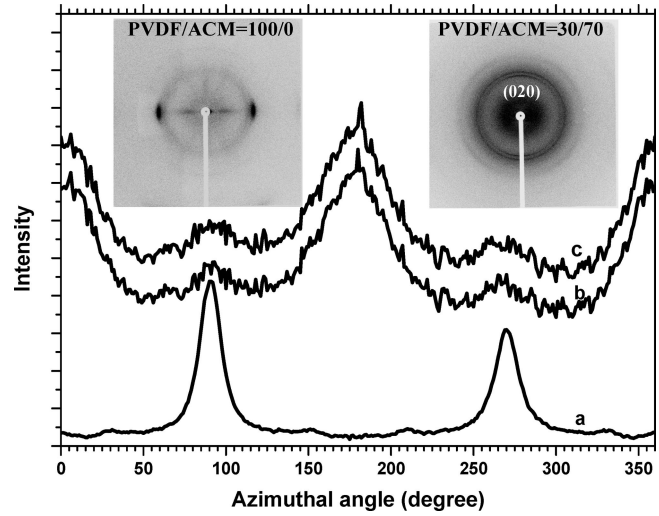

Figure 4. Azimuthal profiles of stretched (a) PVDF ((110/020) diffractions), (b) PVDF/ACM = 20/80 ((020) diffraction), and (c) PVDF/ACM = 30/70 ((020) diffraction). The insets are the WAXD patterns of neat PVDF and the PVDF/ACM = 30/70 blend.

samples, however, a pair of reflection arches at 2θ = 18.8° ((020) reflection of α crystals) is observed in the meridian direction, while no reflections appear on the equator. The reflection peaks are only located at ϕ = 0 and 180° in its azimuthal profiles. In addition, the (110) reflection of PVDF α crystals forms arches in the WAXD pattern in Figure 4. These results indicate that PVDF crystals retain the α-phase during stretching and that the PVDF crystal *b*-axis is oriented along the stretch direction.

It is very interesting to find that the PVDF crystals show totally different orientation behaviors upon stretching in neat PVDF and in PVDF/ACM blends investigated here. The PVDF α-phase is transformed into the β-phase upon stretching, and the molecular chain is also oriented parallel to the stretching direction in the neat PVDF sample. However, the PVDF crystals in the blends have no strain-induced phase transitions behaviors, and the crystal molecular chain is perpendicular to the stretching direction. We attribute this significant difference to the presence of tie molecules. Huang and Brown[11] have proposed an equation to estimate the tie molecule fraction (*P*) for a neat crystalline polymer. For a miscible crystalline/amorphous polymer blend, the equation can be simply modified as follows:

$$P = \frac{1}{3}\frac{\int_L^\infty r^2 \exp(-b^2 r^2)\,dr}{\int_0^\infty r^2 \exp(-b^2 r^2)\,dr}\chi \qquad (1)$$

where *L* is the critical distance required to form a tie molecule, *r* is the probability of a given end-to-end distance, $b^2 = 3/2\bar{r}^{-2}$ ($\bar{r}$ is the root-mean-square value of the end-to-end distance of a random coil), and χ is the volume fraction for the crystalline component in the miscible blends. To build up intercrystalline tie molecules, the chain segments have to be long enough to span an amorphous layer and the two adjacent crystalline lamellae, that is, chain segments longer than critical distance $L = 2L_c + L_a$, where L_c is the crystal lamellar thickness and L_a is the amorphous layer thickness. The calculated results for neat PVDF and the blends are shown in Table 1. It is seen that the tie molecule fraction in the blend is much lower than that in neat PVDF. It is clear that, for neat PVDF, many PVDF molecules in the amorphous part are trapped into the crystal lamellae and therefore function as tie molecules to connect the different crystal lamellae. These tie molecules will transfer the

Table 1. Tie Molecule Fraction (*P*) Calculated from the Brown Equation

sample	neat PVDF	PVDF/ACM = 30/70	PVDF/ACM = 20/80	PVDF/ACM = 10/90
P	0.257	0.034	0.022	0.011

stress from the amorphous part to the crystalline part very effectively during stretching. Before stretching, PVDF crystallizes into the normal α-phase, where the chain takes the conformation of alternating *trans* and *gauche* sequences, or TGTG^-.[34] Upon stretching, these tie molecules become tensioned first and then transfer the applied stress effectively to polymer crystallites.[35] The stress renders the chain conformation in the crystals to the all-trans planar zigzag conformation,[35] and the PVDF crystals transformed into the *β*-phase. At the same time, the deformation by the stretching induces the fibrillar transformation of PVDF crystals. The fibrillar transformation draws the chains along the stretch axis, and the crystal blocks are then normal to the stretch direction.[36] On the other hand, for the PVDF crystals in the ACM-rich blend, a large number of ACM molecule chains are inserted into the gallery of the PVDF lamellae, as confirmed by the more than 2 times increase in crystal long period. The inserted ACM chains separate the crystallite into individual lamella, and few PVDF tie molecules exist between the crystallites. No crystal form transition can be observed since the applied stress cannot be effectively transferred into the PVDF crystals due to the lack of connections between the crystallites. In other words, owing to the very low concentration of tie chain molecules in the ACM-rich blends, the integrity of the PVDF crystal lamellae embedded in the soft ACM matrix is preserved. The tensile loading is mainly exerted on the AMC matrix. As stretching proceeds, the rubbery ACM matrix of the blends flows under the applied tensile stress and the elongated crystallites orient themselves along the flow lines (i.e., the stretching direction) due to the viscous forces from the matrix. Therefore, the long axis of the embedded PVDF crystallites in the network will be rendered to align along the stretching direction. The previous literatures have reported that crystallites of α-PVDF grow preferentially in the direction of the crystallographic *b*-axis.[37] Moreover, it is generally accepted that the longer dimension of crystals should be the crystal growth direction. Therefore, PVDF crystal *b*-axis oriented texture is observed from the WAXD pattern in the blends. A schematic diagram for the stretching process of PVDF crystals with tie molecules in neat PVDF and with few tie molecules in the PVDF/ACM blends is shown in Figure 5.

Figure 6 shows the stress−strain curves of the PVDF/ACM = 20/80 and 30/70 blends. The stress increases slowly with increasing the applied strain, and higher PVDF loading results in higher strength and modulus. However, no strain-hardening behavior up to break was observed for both samples. This mechanical deformation behavior supports our analysis that the investigated ACM-rich blends have very low concentration of tie molecules.

In summary, we reported a type of polymer crystallite with very low concentration of tie chain molecules from a miscible amorphous/crystalline polymer blend for the first time. The PVDF crystallites were simply embedded in the ACM matrix with few molecular connections. Therefore, in contrast to crystallites with tie molecules, no plastic deformation occurs under tensile loading for these crystallites in the blends. Thereby, no strain-induced phase transition was observed for the PVDF crystals in the blends. Furthermore, different from the normal *c*-axis orientation textures, the PVDF crystal lamellae were aligned with *b*-axis along the stretch direction upon stretching. The detailed investigation of the crystallization and melting behaviors as well as the crystal thickening behavior upon annealing is currently underway and will be reported soon.

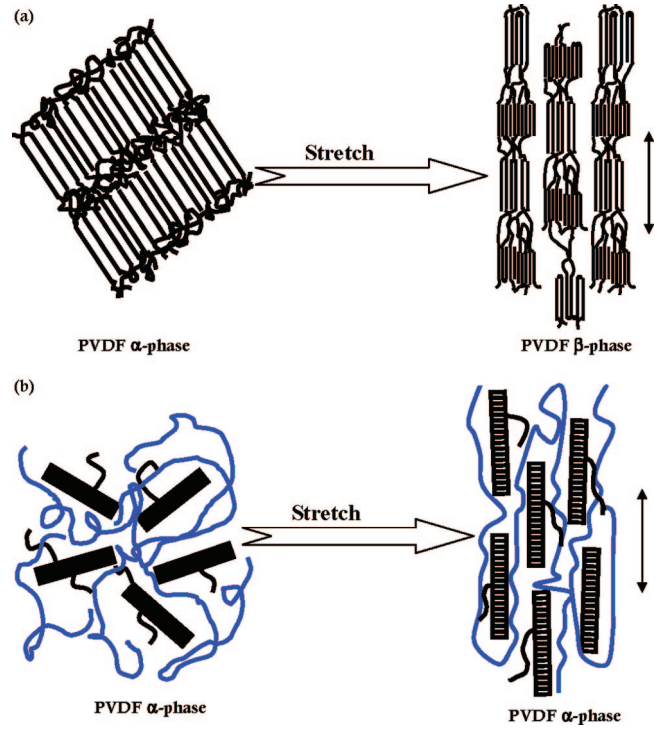

Figure 5. Schematic diagram upon stretching for (a) PVDF crystals with tie molecules in neat PVDF and (b) PVDF crystals with few tie molecules in PVDF/ACM blends. The arrows show the stretching direction. The blue line in (b) indicates the ACM molecular chain.

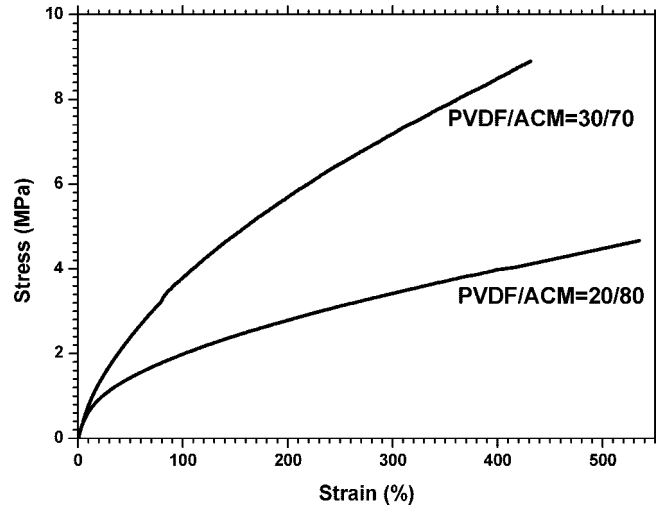

Figure 6. Stress−strain curves for the PVDF/ACM blends with few tie molecules.

Acknowledgment. This work is supported by the New Energy and Industrial Technology Development Organization (NEDO) for the "Project on the Nanostructured Polymeric Materials". The authors thank the reviewers for valuable suggestions.

Supporting Information Available: Figures showing the DMA and DSC profiles and table giving the thermal parameters. This material is available free of charge via the Internet at http://pubs.acs.org.

References and Notes

(1) Keith, H. D.; Paden, F. J., Jr.; Vadimsky, R. G. *J. Polym. Sci., Part A-2: Polym. Phys.* **1966**, *4*, 267.
(2) Friedrich, K. *Adv. Polym. Sci.* **1983**, *52*, 225.

(3) Shah, A.; Stepanov, E. V.; Capaccio, G.; Hiltner, A.; Baer, E. *J. Polym. Sci., Part B: Polym. Phys.* **1998**, *36*, 2355.
(4) Seguela, R. *J. Polym. Sci., Part B: Polym. Phys.* **2005**, *43*, 1729.
(5) Porter, R. S.; Johnson, J. F. *Chem. Rev.* **1966**, *66*, 1.
(6) Fischer, E. W. *Pure Appl. Chem.* **1978**, *50*, 1319.
(7) Darras, O.; Seguela, R. *Colloid Polym. Sci.* **1995**, *273*, 753.
(8) Peterlin, A. *J. Macromol. Sci., Phys.* **1973**, *7*, 705.
(9) Brown, N.; Ward, I. M. *J. Mater. Sci.* **1983**, *18*, 1405.
(10) Haward, R. N. *J. Polym. Sci., Part B: Polym. Phys.* **1995**, *33*, 1481.
(11) (a) Huang, Y. L.; Brown, N. *J. Mater. Sci.* **1988**, *23*, 3648. (b) Huang, Y. L.; Brown, N. *J. Polym. Sci., Part B: Polym. Phys.* **1990**, *28*, 2007. (c) Huang, Y. L.; Brown, N. *J. Polym. Sci., Part B: Polym. Phys.* **1991**, *29*, 129.
(12) Lustiger, A.; Ishikawa, N. *J. Polym. Sci., Part B: Polym. Phys.* **1991**, *29*, 1047.
(13) Uehara, H.; Matsuda, H.; Aoike, T.; Yamanobe, T.; Komoto, T. *Polymer* **2001**, *42*, 5893.
(14) Zhang, M. Z.; Yuen, F.; Choi, P. *Macromolecules* **2006**, *39*, 8517.
(15) Shen, F. W.; McKellop, H. A.; Salovey, R. *J. Polym. Sci., Part B: Polym. Phys.* **1996**, *34*, 1063.
(16) Nitta, K. H.; Takayanagi, M. *J. Polym. Sci., Part B: Polym. Phys.* **1999**, *37*, 357.
(17) Takayanagi, M.; Nitta, K. *Macromol. Theory Simul.* **1997**, *6*, 181.
(18) Stein, R. S.; Khambatta, F. B.; Warner, F. P.; Russell, T. P.; Escala, A.; Balizer, E. *J. Polym. Sci., Polym. Symp.* **1978**, *63*, 313.
(19) Chen, H. L.; Wu, S. F.; Lin, T. L.; Wu, G. M. *Polym. J.* **2002**, *34*, 356.
(20) Vanneste, M.; Groeninckx, G.; Reynaers, H. *Polymer* **1997**, *38*, 4407.
(21) Chen, H. L.; Wang, S. F.; Lin, T. L. *Macromolecules* **1998**, *31*, 8924.
(22) Zhang, X. Q.; Takegoshi, K.; Hikichi, K. *Macromolecules* **1992**, *25*, 2336.
(23) Chen, H. L.; Li, L. J.; Lin, T. L. *Macromolecules* **1998**, *31*, 2255.
(24) Nishi, T.; Wang, T. T. *Macromolecules* **1975**, *8*, 909.
(25) Morra, B. S.; Stein, R. S. *J. Polym. Sci., Part B: Polym. Phys.* **1982**, *20*, 2243.
(26) Bernstein, R. E.; Paul, D. R.; Barlow, J. W. *Polym. Eng. Sci.* **1978**, *18*, 683.
(27) Ellis, T. S. *Macromolecules* **1989**, *22*, 743.
(28) Persyn, O.; Miri, V.; Lefebvre, J. M.; Depecker, C.; Gors, C.; Stroeks, A. *Polym. Eng. Sci.* **2004**, *44*, 261.
(29) Aubin, M.; Prud'homme, R. E. *Macromolecules* **1980**, *13*, 365.
(30) Matsushige, K.; Nagata, K.; Imada, S.; Takemura, T. *Polymer* **1980**, *21*, 1391.
(31) Wu, J.; Shultz, J. M.; Yeh, F. J.; Hsiao, B. S.; Chu, B. *Macromolecules* **2000**, *33*, 1765.
(32) Sajkiewicz, P.; Wasiak, A.; Goclowski, Z. *Eur. Polym. J.* **1999**, *35*, 423.
(33) Hsu, T. G.; Geil, P. H. *J. Mater. Sci.* **1989**, *24*, 1219.
(34) Takahashi, Y.; Matsubara, Y.; Tadokorao, H. *Macromolecules* **1983**, *16*, 1588.
(35) Hasegawa, R. *Polym. J.* **1972**, *3*, 600.
(36) Peterlin, A. *J. Mater. Sci.* **1971**, *6*, 490.
(37) (a) Lovinger, A. J.; Wang, T. T. *Polymer* **1979**, *20*, 725. (b) Lovinger, A. J. *J. Polym. Sci., Polym. Phys.* **1980**, *18*, 739.

MA800148X